Macromolecules

pubs.acs.org/Macromolecules Article

Cationic, Anionic, and Amphoteric Dual pH/Temperature-Responsive Degradable Microgels via Self-Assembly of Functionalized Oligomeric Precursor Polymers

Eva Mueller, Sebastian Himbert, Madeline J. Simpson, Markus Bleuel, Maikel C. Rheinstadter, and Todd Hoare*

Cite This: *Macromolecules* 2021, 54, 351−363 Read Online

ACCESS | Metrics & More | Article Recommendations | Supporting Information

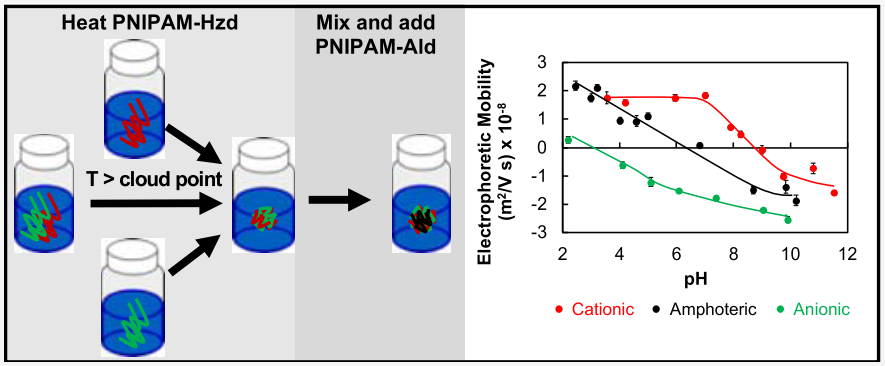

ABSTRACT: Multiresponsive smart materials with the capacity to reversibly change properties (i.e., size, charge) upon the application of more than one stimulus (i.e., temperature, pH) offer potential in numerous biotechnology and biomedical applications. However, their typical lack of degradability limits their potential *in vivo* use. Herein, we demonstrate the use of an aqueous thermally driven self-assembly approach based on hydrazide- and aldehyde-functionalized poly(*N*-isopropylacrylamide) (PNIPAM) oligomers functionalized with pH-ionizable cationic or anionic comonomers for fabricating degradable temperature/pH dual-responsive microgels. The self-assembled microgels show properties analogous to conventional cationic or anionic PNIPAM microgels, retaining their thermal responsiveness while exhibiting pH-driven swelling upon functional comonomer ionization. Amphoteric microgels can also be produced by mixing cationic- and anionic-functionalized precursor polymers during the self-assembly process that reproduce the high-pH/low-pH parabolic swelling response observed in conventional amphoteric microgels. Coupling the precise dual-responsive swelling responses achievable with the degradability of the hydrazone cross-links, self-assembled charged PNIPAM microgels offer potential for improved performance in drug delivery applications requiring dual pH/temperature-specific delivery (e.g. infection sites or cancer).

INTRODUCTION

Stimulus-responsive or "smart" polymers are increasingly attracting interest in biotechnology and medicine given their capacity to quickly and reversibly switch their physical properties when exposed to small changes in their physical (e.g., temperature, light, electromagnetic fields) or chemical (pH, ionic strength, specific target chemicals) environments.[1−3] Smart hydrogels are particularly attractive given that dynamic changes in the mesh size of the gel network can be engineered using the smart switch, enabling dynamic control over drug release kinetics from the hydrogel.[4,5] Microgels, hydrogel nanoparticles on the size range of 10 nm to 1 μm,[6] offer further advantages in the context of drug delivery in terms of their faster responses to external stimuli, minimally invasive administration due to their nanoscale size, and potential for long circulation times *in vivo* given their high water content and thus low interfacial tension.[7−9]

Thermoresponsive poly(*N*-isopropylacrylamide) (PNIPAM) microgels are perhaps the best-known smart soft nanomaterial, showing a volume phase transition temperature (VPTT) of ∼32 °C above which they discontinuously shrink in size.[10−12] Due to their high blood plasma stability, typically narrower size dispersity, and more adaptable chemistries relative to other

Received: October 8, 2020
Revised: December 11, 2020
Published: December 29, 2020

https://dx.doi.org/10.1021/acs.macromol.0c02304
Macromolecules 2021, 54, 351−363

carriers such as liposomes or micelles, PNIPAM microgels have been widely investigated as a drug delivery vehicle, particularly for anticancer drugs given that their small tunable size (<200 nm) allows for efficient circulation and cell uptake.[13−15] In addition, copolymerization of NIPAM with various functional monomers (e.g., acrylic acid,[16−19] methacrylic acid,[20−22] maleic acid,[23] vinylacetic acid,[24] allylacetic acid,[25] and dimethylaminoethyl methacrylate[26]) can introduce pH-responsive functional groups into the network that enable the particles to exhibit dual pH/temperature smart responses of potential utility for physically targeting specific disease sites characterized by both higher local temperatures and lower local pH values (e.g., inflammation sites or tumors).[15,24,27−29] As such, developing clinically relevant microgel compositions with the potential for dual pH/temperature responsiveness offers promise for addressing the key targeting challenges that currently limit the impact of nanomedicines in the clinic.[10,30,31]

Conventional PNIPAM microgels are prepared via a free-radical precipitation polymerization strategy in which the phase transition of PNIPAM is exploited to first create nucleation sites and then grow the microgel particles as polymerization proceeds.[12] While this strategy facilitates the production of high yields of typically highly monodisperse microgels, the degradability of the microgels produced is ill-defined. Most microgel preparations use a nondegradable cross-linker; even if the cross-linker is degradable, the molecular weights of the degradation products are typically not controllable and thus may not be cleared following gel degradation. Chain transfer reactions can also occur that create additional C−C bonds in addition to the degradable cross-linking points (enabling microgels to be formed even if no cross-linker is added[32,33]), further limiting the potential of the microgel to degrade into renally clearable units. To address this degradability issue, a thermally driven oligomer self-assembly approach has recently been developed in our group.[34] In this method, a hydrazide-functionalized PNIPAM precursor polymer with a molecular weight below the renal cutoff is heated above its cloud point to form un-cross-linked but well-defined nanoaggregates. Upon the addition of an aldehyde-functionalized PNIPAM precursor polymer with a similarly low molecular weight, an acid-labile hydrazone bond is formed between the hydrazide and aldehyde groups to fabricate microgels. These microgels are degradable, monodisperse, and colloidally stable while exhibiting analogous temperature-responsive properties to conventional precipitation-based PNIPAM microgels. In addition, while conventional microgels have a dense core/diffuse shell structure regulated by the copolymerization kinetics of the cross-linker and NIPAM, self-assembled microgels have a homogeneous internal structure of potential benefit for regulating drug release.[35] However, for this method to be broadly useful for *in vivo* drug delivery, the integration of functional groups to enable improved drug uptake, targeting, and multistimulus response properties is required.

Herein, we demonstrate the fabrication of dual temperature/pH-responsive microgels by incorporating charge into the precursor polymers used for the self-assembly. In particular, by using mixtures of precursor polymers with different types and degrees of functionalization, we show the potential to fabricate cationic, anionic, and amphoteric microgels with well-defined charge densities by simple mixing of different ratios of cationic, anionic, and neutral precursor polymers during the assembly process. Amphoteric microgels, which have previously been fabricated using conventional precipitation polymerization,[36−38] offer particular interest given the superior repellency of many amphoteric polymers to protein adsorption (key for promoting long circulation times *in vivo*) as well as their unique pH swelling/deswelling behaviors and charge switching capacity that enables reversible scavenging of biomolecules,[39] effective nanoparticle sequestration,[40] and pH-switchable biomolecule loading/release (e.g., of DNA for gene delivery[39]). We assess both the capacity of our self-assembly technique to make well-controlled charged microgels and the effect of charge on the morphologies of the self-assembled microgels using small-angle neutron scattering, the latter to determine whether the homogeneous internal microstructures observed with the neutral self-assembled microgels are maintained when charged precursor polymers are used in the self-assembly process. To the best of our knowledge, this is the first report using an oligomeric self-assembly technique to fabricate pH-ionizable degradable microgels yielding well-defined degradation products.

EXPERIMENTAL SECTION

Materials. *N*-Isopropylacrylamide (NIPAM, 99%), acrylic acid (AA, 99%), 2-(dimethylamino) ethyl methacrylate (DMAEMA, 98%), thioglycolic acid (TGA, 98%), aminoacetaldehyde dimethyl acetal (99%), sodium cyanoborohydride (95%), 2,2,6,6-tetramethyl-1-piperidinyloxy (TEMPO, 98%), methacryloyl chloride (purum), acryloyl chloride (97%), triethylamine, and tert-butyl carbazate (98%) were purchased from Sigma-Aldrich (Oakville, ON). NIPAM was purified by dissolving 1 g/mL in toluene at 60 °C, adding a 2:3 ratio of hexane to toluene, placing the solution in an ice bath for 1−2 h, filtering/rinsing with hexanes, and drying the recrystallized NIPAM monomer under N_2 overnight. Adipic acid dihydrazide (ADH, Alfa Aesar, 98%), *N*′-ethyl-*N*-(3-dimethylaminopropyl)-carbodiimide (EDC, Carbosynth, Compton CA, commercial grade), 2,2-azobisisobutyric acid dimethyl ester (AIBMe, Wako Chemicals, 98.5%), and ethanol (Commercial Alcohols, Brampton, ON) were purchased and used without further purification. Milli-Q grade distilled deionized water (DIW) was used for all experiments.

Hydrazide Acrylate Monomer Synthesis. The hydrazide acrylate monomer (*tert*-butyl-2-acryloylhydrazine-1-carboxylate) was synthesized by adding triethylamine (2.40 mL, 17.3 μmol, 1.1 equiv) to a solution of boc-carbazate (2.07 g, 15.7 μmol) in CH_2Cl_2 (75 mL) under a nitrogen atmosphere and then cooling the solution to 0 °C. Acryloyl chloride (1.27 mL, 15.7 μmol) was added dropwise over 5 min, and the reaction was allowed to stir at 0 °C for 30 min. Following, the crude reaction mixture was filtered to remove the triethylamine hydrochloride salt and the filtrate was concentrated by rotary evaporation. The product was purified via silica gel column chromatography (2:1 to 1:1 Hex/EtOAc) to give 1.52 g of the desired product (52% yield). The ^{1}H NMR spectra confirming the successful synthesis of the monomer are provided in the Supporting Information Figure S1.

Prepolymer Synthesis. All polymers were prepared via free-radical copolymerization of NIPAM (4.5 g) in 20 mL of ethanol using thioglycolic acid (TGA, 80 μL) as the chain transfer agent and 2,2-azobisisobutyric acid dimethyl ester (AIBME, 0.056 g) as the initiator (reaction temperature = 60 °C).

Cationic Hydrazide-Functionalized PNIPAM ((+)-PNIPAM-Hzd). The base recipe was used together with 0.5 g AA and 2 mL DMAEMA. The acrylic acid residues were subsequently converted to hydrazide groups by dissolving 1 g of PNIPAM-*co*-AA−DMAEMA, 20 g of adipic acid dihydrazide (ADH, 5-fold molar excess), and 11 g of EDC in 200 mL of Milli-Q water. The pH was adjusted to 4.75 and maintained throughout the reaction (4−5 h) via the addition of 1 M HCl as required to facilitate the conjugation of ADH to the acrylic acid residues. The resulting solution was dialyzed against Milli-Q water over six 6 h cycles (12−14 kDa MWCO) and lyophilized for dry storage. Conductometric titration indicated that 95 mol % of

https://dx.doi.org/10.1021/acs.macromol.0c02304
Macromolecules 2021, 54, 351−363

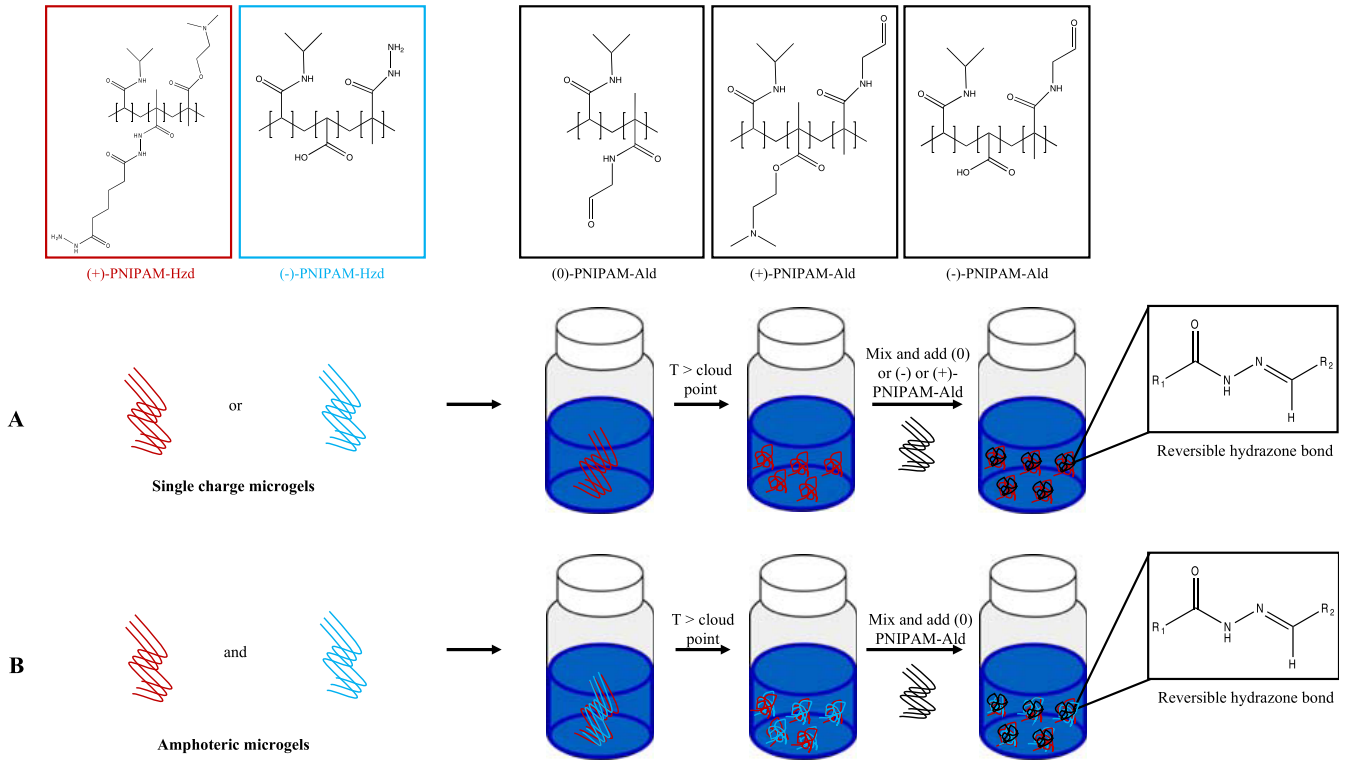

Figure 1. Schematic for (A) single-charge microgel self-assembly and (B) amphoteric microgel self-assembly illustrating the seed polymer blending technique used to control relative charge, including the chemistry of the hydrazide and aldehyde-functionalized polymers and reversible aldehyde−hydrazide chemistry used in the self-assembly process.

acrylic acid monomer units in the polymer were hydrazide-functionalized.

Anionic Hydrazide-Functionalized PNIPAM ((−)PNIPAM-Hzd). The base recipe was used together with 1.3 g of the hydrazide acrylate monomer and 0.5 g of AA. After the overnight polymerization, the polymer was dissolved in 5 mL of a 50:50 DCM:TFA mixture for 2−3 h to remove the *t*-butyl protecting group and expose the hydrazide group. Once the solvent was blown off with air in the fumehood overnight, the polymer was dissolved in water and dialyzed over six cycles against Milli-Q water using a 12−14 MWCO membrane and lyophilized to dryness for storage.

Cationic Aldehyde-Functionalized PNIPAM ((+)-PNIPAM-Ald). The base recipe was used together with 2.1 mL of DMAEMA and 0.95 g of *N*-(2,2-dimethoxyethyl)methacrylamide (DMEMAm). After the overnight polymerization, the polymer was dissolved in 1 M HCl for 24 h to hydrolyze the pendant acetal group in DMEMAm into aldehyde groups. The resulting solution was dialyzed against Milli-Q water over six 6 h cycles using a 12−14 kDa MWCO membrane and lyophilized to dryness for storage.

Anionic Aldehyde-Functionalized PNIPAM ((−)-PNIPAM-Ald). The base recipe was used together with 0.5 g of AA and 0.95 g of *N*-(2,2-dimethoxyethyl)methacrylamide (DMEMAm). Polymerization and workup were conducted analogously to that described for the cationic PNIPAM-Ald polymer.

Prepolymer Characterization. Base-into-acid conductometric titration (ManTech Associates) using 0.1 M NaOH as the titrant and 50 mg of the functionalized microgel suspended in 1 mM NaCl as the sample was used to measure the stoichiometric incorporation of the titratable comonomers AA and DMAEMA (mol %) into the polymer as well as before and after ADH functionalization to identify the efficiency of hydrazide functionalization for (+)-PNIPAM-Hzd. Nuclear magnetic resonance (^{1}H NMR, Bruker AV600 in d_6-DMSO) was used to confirm the identity and composition of the hydrazide acrylate monomer as well as the copolymers. Gel permeation chromatography using a Waters 590 HPLC pump, three Waters Styragel columns (HR2, HR3, HR4; 30 cm × 7.8 mm (i.d.); 5 μm particles) maintained at 40 °C, a Waters 410 refractive index detector operating at 35 °C, and DMF as the solvent was used to measure the molecular weight of the precursor polymers.

Cloud Point Measurements. The cloud point of the functionalized PNIPAM polymers was measured using UV−vis spectrophotometry (Varian Cary Bio 100). Transmittance and absorbance measurements were performed over a temperature range of 25−80 °C (2 °C intervals, 1 °C/min ramp rate), with the onset cloud point defined as the temperature at which the transmittance of the sample was 95%.

Microgel Fabrication. To fabricate neutral or single-charge microgels, hydrazide-functionalized PNIPAM polymer (with or without cationic or anionic charge) was dissolved at 1 wt % in 5 mM NaCl, adjusted to the target assembly pH using 0.1 M NaOH or 0.1 M HCl, and heated to 5 °C+ cloud point (based on the onset cloud point measured via UV−vis spectrophotometry). The precursor polymer switched from transparent to cloudy, confirming the generation of nanoaggregates upon heating. Upon this phase change (~3−5 min), the aldehyde-functionalized polymer (dissolved in 1 wt % in water but without pH adjustment) was added dropwise over 1−2 min, after which the reaction was allowed to continue for 15 min in the heated oil bath. A cross-linker:seed polymer (Ald:Hzd) mass ratio of 0.2 was used for all assemblies, consistent with previous studies that indicated that this ratio of cross-linker:seed polymer yielded microgels with the best monodispersity.[34]

To fabricate amphoteric microgels, cationic and anionic PNIPAM-Hzd polymers were mixed at the desired charge ratio of the final microgel while maintaining the same overall mass concentration (1 wt %) used for the single-charge microgels and 5 mM NaCl as the assembly solvent (with suitable pH adjustment per the target assembly conditions) to partially screen the opposite charges in the prepolymer solution and avoid microscopic coacervate formation. Assembly was conducted as described for the single-charge microgels using neutral PNIPAM-Ald as the cross-linker (Figure 1).

Microgel Characterization. Particle size was measured by dynamic light scattering using a Brookhaven 90Plus particle analyzer

https://dx.doi.org/10.1021/acs.macromol.0c02304
Macromolecules 2021, 54, 351−363

running Particle Solutions Software (Version 2.6, Brookhaven Instruments Corporation) with a 659 nm laser and a 90° detection angle. Each measurement was performed at a count rate between 200 and 500 kilocounts/s for 2 min, and all microgels were measured in 5 mM NaCl with pH values adjusted using 0.1 M NaOH and 0.1 M HCl. The intensity-weighted particle sizes and polydispersities were reported as averages of the six replicate measurements, with the reported error representing the standard deviation of these replicates. Electrophoretic mobility was measured using a ZetaPlus ζ-potential analyzer (Brookhaven Instrument Corporation) operating in phase analysis light scattering (PALS) mode. Samples were prepared in 5 mM NaCl and tested in triplicate, with each run consisting of 15 cycles; the experimental uncertainties represent the standard deviation of the replicate measurements. Both the diameter and the ζ-potential/mobility of the microgels were investigated as a function of pH, with 0.1 M NaOH and 0.1 M HCl used to adjust the pH as required. Microgel degradation was measured by adding a volume of 5 mL of 1 M hydrochloric acid to 1 mL of a 10 mg/mL microgel suspension and tracking the particle size as a function of time using dynamic light scattering as described above. As additional confirmation, gel permeation chromatography was conducted using an Agilent 1260 infinity II GPC system with an Agilent 1260 infinity RI detector (controlled at 30 °C) and a Superpose 6 increase 10/300 GL (GE healthcare) column. The solvent was 1× PBS with 0.05% sodium azide at a flow rate of 0.5 mL/min, and the system was calibrated with narrow PEG standards from 3 to 60 kDa. The degradation products following 24 h of treatment with 1 M HCl were also assessed to determine the efficacy of the breakdown of the microgels into their precursor polymer components.

Small-Angle Neutron Scattering (SANS). SANS experiments were conducted using the 30 m SANS NGB30 at the NIST Center for Neutron Research (NCNR, Gaithersburg, MD).[41] Sample-to-detector distances of 1 and 4 m with a neutron wavelength of 6 Å were used together with the 13 m lens configuration of the instrument with a neutron wavelength of 8.4 Å to measure a q range between 0.001 and 1 $Å^{-1}$. The microgels were self-assembled in D_2O and loaded into NCNR's custom titanium/quartz sample holders (diameter 19 mm and thickness 2 mm, corresponding to a volume of ~800 μL per sample). The low q range data were acquired by counting for ~20 min using the 13 m distance, the medium q range data were acquired by counting for ~15 min using the 4 m distance, and the high q range data were acquired for ~5 min using the 1 m detection distance. The three ranges were reduced and merged using Igor Pro Version 6.37 and macros provided by NCNR.[42,43]

Ultrasmall-Angle Neutron Scattering (USANS). USANS experiments were conducted on the microgels using the BT5 USANS at the NIST Center for Neutron Research (NCNR, Gaithersburg, MD).[44] The neutron wavelength used was 2.4 Å ± 6%, with the q range spanning between ~0.00003 and 0.002 $Å^{-1}$ to overlap the lower end of the accessible q range from SANS (0.001 $Å^{-1}$). The data were reduced and merged using Igor Pro Version 6.37 and macros provided by the NCNR.[42,43]

Neutron Scattering Data Analyses. Data corresponding to all single-charged self-assembled PNIPAM microgel samples were fitted using a fuzzy sphere model with an additional Ornstein−Zernike Lorentzian term, as has been previously used for neutral self-assembled PNIPAM microgels[35]

$$I(q) = \frac{\text{scale}}{V}(\Delta p)^2\langle A^2(q)\rangle S(q) + \frac{L}{1+(\xi q)^m} + bkg$$

$$A(q) = \frac{3[\sin(qR) - qR\cos(qR)]}{(qR)^3}\exp\left(\frac{-(\sigma_{\text{fuzzy}}q)^2}{2}\right)$$

Here, R is the mean radius of the sphere, L is the scale of the Lorentzian, ξ is the Lorentzian correlation length, and m is the Lorentzian exponent. The fuzziness σ_{fuzzy} was set to 0 for all fits, reducing the expression to that of a homogeneous sphere.

For amphoteric self-assembled microgels whose scattering profile does not fit the Lorentzian model, a weak interaction was introduced to the model as a square well potential[45]

$$U(q) = \begin{cases} \infty & r < 2R \\ -\varepsilon & 2R \le r \le 2R\alpha \\ 0 & r > 2R\alpha \end{cases}$$

where ε is the well depth, α is the well width, and R is the particle size. The square well potential is a representation of the Coulombic potential, in which the well depth represents the strength of the electric potential between two incompressible spheres and the well width is the probability of this interaction. The combined structure factor is then defined as the product of the structure factor of a fuzzy sphere (as described above) and the structure factor of a square well potential fluid as described in Sharma el al.[45]

Cell Cytotoxicity Experiment. The MTS cell proliferation colorimetric assay kit (BioVision) was used to test the cell viability in the presence of the charged self-assembled PNIPAM microgels. C2C12 myoblast cells were cultured at 1×10^4 cells/well in a 96-well plate with a volume of 150 μL DMEM/well without any additional factors for 24 h, after which the charged self-assembled PNIPAM microgels were added at each specific concentration to increase the final volume to 200 μL/well. The plates were then incubated for 24 h until 20 μL of MTS reagent was added to each well and incubated for 2 h at 37 °C in standard culture conditions. The absorbance of the treated and untreated cells was measured using a plate reader operating at 490 nm.

RESULTS AND DISCUSSION

Polymer Characterization. Conductometric titration data measuring the concentration of anionic or cationic comonomer incorporated into the charged precursor PNIPAM polymers is summarized in Table 1.

Table 1. Charged PNIPAM Polymer Characterization

polymer	mol % charged comonomer incorporation	M_n (kDa)	PD
(+)-PNIPAM-Hzd	19 ± 2	15.8	1.3
(−)-PNIPAM-Hzd	17 ± 3	14.3	1.4
(+)-PNIPAM-Ald	21 ± 1	17.2	1.9
(−)-PNIPAM-Ald	17 ± 2	16.7	1.7

Each charged polymer was successfully functionalized with close to the target (20 mol %) cationic or anionic functional comonomer; as such, mass-by-mass mixing of the polymers (in particular, the two hydrazide polymers used for fabricating amphoteric microgels) will yield near-stoichiometric charge balances. These numbers are consistent with the ^{1}H NMR spectra of these polymers (Supporting Information Figures S2−S5), which confirm the incorporation of functional monomer as well as the appropriate reactive functional groups for enabling cross-linking. All polymers also have a very similar molecular weight well below the renal cutoff (<40 kDa), permitting facile mixing of the polymers as well as clearance of the degradation products resulting from microgels prepared with any combination of the precursor polymers. The percentage of the precursor polymer mass incorporated into microgels (47−62% depending on the composition used; Table S1) is slightly lower than typically observed with unfunctionalized conventional precipitation-based microgels (70−80%[46,47]); however, the incorporation of charged comonomers has less of an impact on the percentage of

https://dx.doi.org/10.1021/acs.macromol.0c02304
Macromolecules 2021, 54, 351−363

polymer mass incorporated into the microgel than is often observed with conventional microgels.[24]

The cloud point values for the seed PNIPAM polymers (1 wt %) at different pH values are summarized in Table 2 (see the Supporting Information Figure S6 for full absorbance versus temperature profiles). The cloud point values for the charged PNIPAM-Ald polymers were included for reference but are not as important to the ultimate success of the self-assembly fabrication process; we have previously demonstrated that the proximity of the self-assembly temperature to the cloud point of the seed (hydrazide-functionalized) precursor polymer(s) is the key driver to forming monodisperse microgels.[48] Given the very high observed cloud point values for the precursor polymers in their charged states, data were collected at different pH values to identify the best pH conditions for enabling self-assembly of the charged precursor polymers.

Table 2. Cloud Points for Functionalized PNIPAM Polymers Measured at Different pH Values

seed polymer	pH 4 (°C)	pH 7 (°C)	pH 10 (°C)
(0)-PNIPAM-Hzd	58	58	58
(−)-PNIPAM-Hzd	52	75	>80
(+)-PNIPAM-Hzd	>80	70	57
(−/+)-PNIPAM-Hzd (1:1)	62	N/A	62
(0)-PNIPAM-Ald	45	45	45
(−)-PNIPAM-Ald	48	55	>80
(+)-PNIPAM-Ald	>80	58	45

When the charged hydrazide precursor polymers were in the ionized state (pH 10 for (−)-PNIPAM-Hzd and pH 4 for (+)-PNIPAM-Hzd), no measurable cloud point was observed up to 80 °C, as the ionization of the functional comonomer shifts the hydrophilic/hydrophobic balance as to make the polymers functionally nonthermoresponsive in water. Conversely, when the charged hydrazide precursor polymers were neutralized (pH 4 for (−)-PNIPAM-Hzd and pH 10 for (+)-PNIPAM-Hzd), measurable cloud point values in the 50−60 °C were observed. A similar general trend was observed with the charged aldehyde precursor polymers, albeit at somewhat lower temperatures corresponding to the reduced hydrogen-bonding potential of aldehyde groups compared to that of hydrazide groups.[49] When the anionic and cationic hydrazide prepolymers were mixed in equal ratios, the cloud points of the overall mixtures are equivalent at both pH 4 ((+)-PNIPAM-Hzd charged, (−)-PNIPAM-Hzd uncharged) and pH 10 ((−)-PNIPAM-Hzd charged, (+)-PNIPAM-Hzd uncharged), consistent with an approximately equal amount of

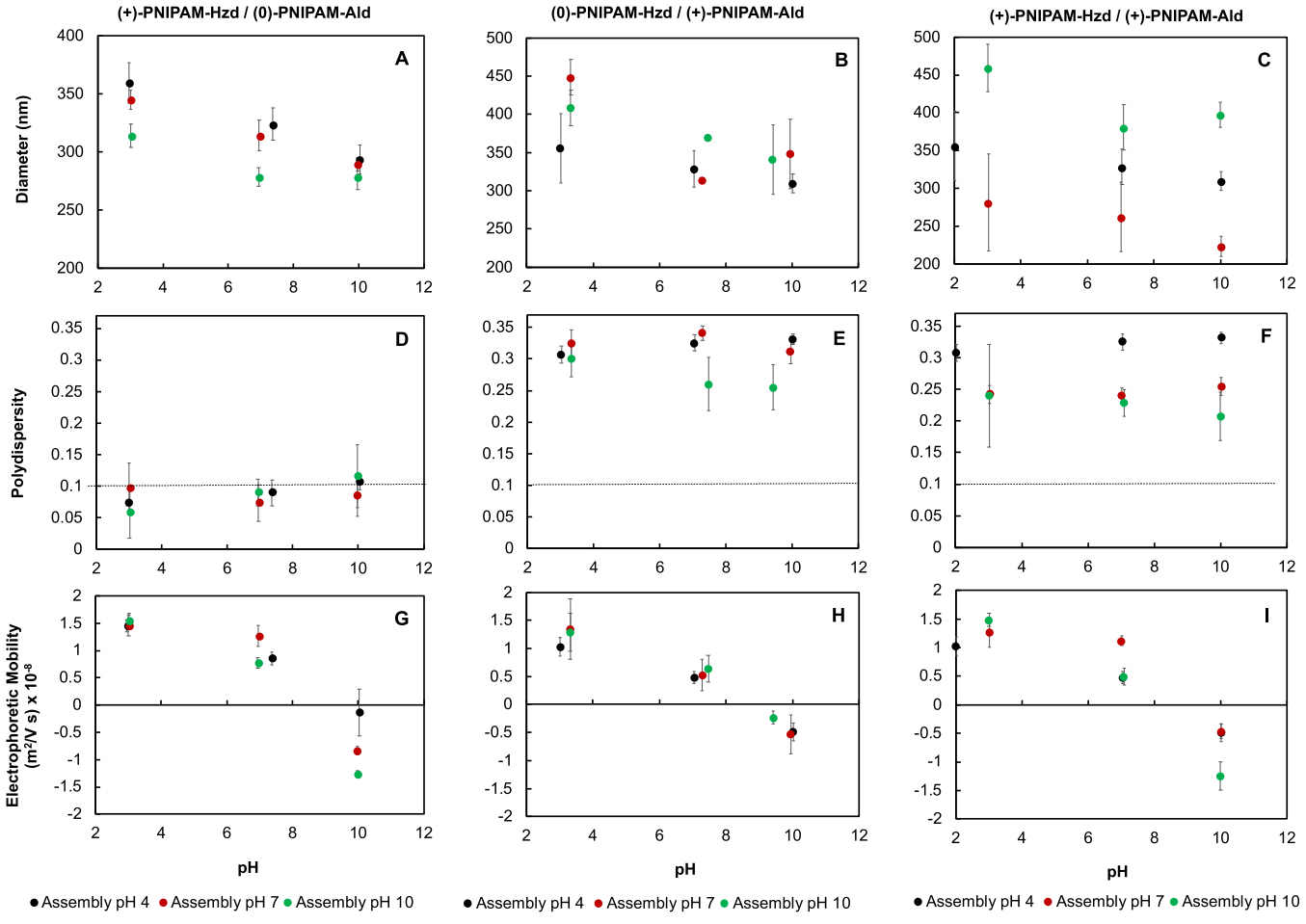

Figure 2. Properties of cationic self-assembled PNIPAM microgels fabricated by mixing (left column, A, D, G) (+)-PNIPAM-Hzd (seed)/(0)-PNIPAM-Ald (cross-linker); (middle, B, E, H) (0)-PNIPAM-Hzd (seed)/(+)-PNIPAM-Ald (cross-linker); (right column, C, F, I) (+)-PNIPAM-Hzd (seed)/(+)-PNIPAM-Ald (cross-linker). The top row (A−C) shows the hydrodynamic diameter, the middle row (D−F) shows the polydispersity, and the bottom row (G−I) shows the electrophoretic mobility, all as a function of pH.

https://dx.doi.org/10.1021/acs.macromol.0c02304
Macromolecules 2021, 54, 351−363

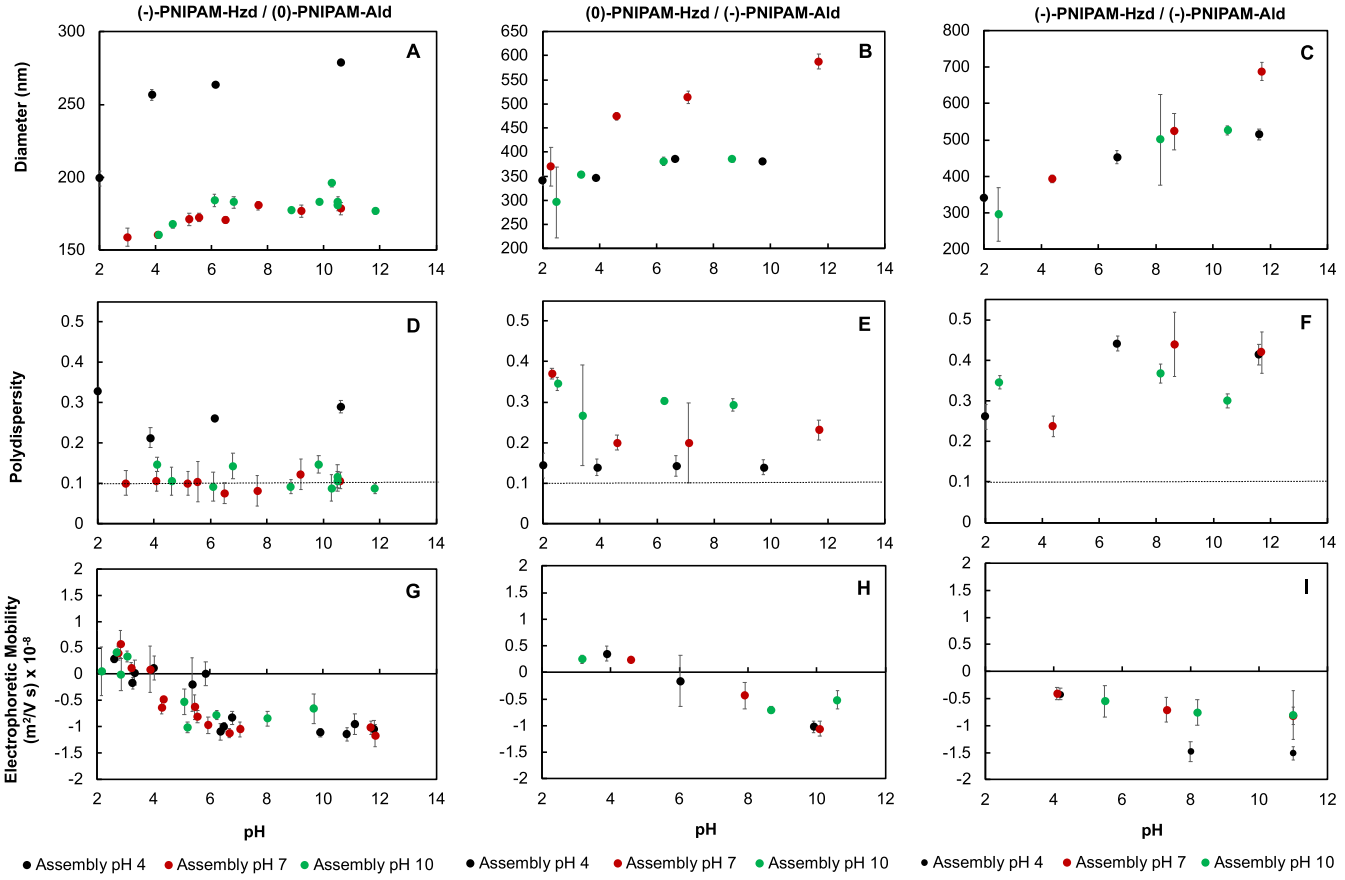

Figure 3. Properties of anionic self-assembled PNIPAM microgels fabricated by mixing (left column, A, D, G) (−)-PNIPAM-Hzd (seed)/(0)-PNIPAM-Ald (cross-linker); (middle, B, E, H) (0)-PNIPAM-Hzd (seed)/(−)-PNIPAM-Ald (cross-linker); (right column, C, F, I) (−)-PNIPAM-Hzd (seed)/(−)-PNIPAM-Ald (cross-linker). The top row (A−C) shows the hydrodynamic diameter, the middle row (D−F) shows the polydispersity, and the bottom row (G−I) shows the electrophoretic mobility, all as a function of pH.

both acidic and basic functional comonomers present in the mixture. Blending of cationic and anionic PNIPAM at pH 7 resulted in macroscopic polymer aggregation such that no cloud point could be measured; no self-assemblies were subsequently performed at this pH value for the amphoteric microgels.

Single-Charge Microgels. *Cationic PNIPAM Microgels.* Three single-charged cationic PNIPAM microgels were fabricated using the described self-assembly protocol, all at a temperature of 5 °C + cloud point of the seed (hydrazide) polymer: (1) (+)-PNIPAM-Hzd/(0)-PNIPAM-Ald (cationic core polymer, neutral cross-linking polymer); (2) (0)-PNIPAM-Hzd/(+)-PNIPAM-Ald (neutral core polymer, cationic cross-linking polymer); and (3) (+)-PNIPAM-Hzd/(+)-PNIPAM-Ald (cationic core and cross-linking polymers). The starting pH was controlled to pH values of 4, 7, and 10 to determine the effects of the starting pH on the final microgel properties. Figure 2 shows the diameter, polydispersity, and electrophoretic mobility as a function of pH for all cationic self-assembled microgels. Note that the particle size of the microgel is governed by the size of the nanoaggregate formed upon heating of the hydrazide-functionalized polymer precursor above its LCST, with the polar hydrazide groups stabilizing the nanoaggregates at a particular size that is then "locked" in place by the addition of the cross-linker (aldehyde-functionalized) polymer. Provided that self-assembly is conducted at a pH value at which the seed (hydrazide) polymer(s) are ionized, the use of charged precursor polymers as the seed both (1) increases the water content of the nanoaggregate and (2) increases the stability of the nanoaggregates due to enhanced electrostatic stabilization; the overall size of each microgel produced thus represents the balance of these competing effects in the nanoaggregate phase.

The hydrodynamic diameter decreased as a function of pH for all cationic microgels tested, consistent with the incorporation of cationic charge into the microgels (the pK_a of DMAEMA is ∼8). Correspondingly, the electrophoretic mobility of the microgels was cationic at acidic pH values and decreased as the pH was increased; the slight negative mobility values observed at highly basic pH values are attributable to charge screening with hydroxyl ions in solution.[50] However, significant differences were observed in the polydispersities and absolute sizes achieved depending on the chemistry and conditions used during the assembly. When the cationic polymer was used only as the seed polymer and a neutral cross-linking polymer was used ((+)-PNIPAM-Hzd/(0)-PNIPAM-Ald), particle sizes were maintained in the 280−360 nm range and polydispersities of <0.1 were consistently achieved at all assembly pH conditions, indicating good monodispersity in the population of fabricated microgels. In comparison, when both the seed polymer and the cross-linking polymer are cationic ((+)-PNIPAM-Hzd/(+)-PNIPAM-Ald), significantly larger polydispersities (0.2−0.35) are observed, particularly at pH 4 at which both polymers are charged and the nanoaggregates are likely to be less clearly defined. Significantly larger effects on particle size as a function of the assembly pH are also

https://dx.doi.org/10.1021/acs.macromol.0c02304
Macromolecules 2021, 54, 351−363

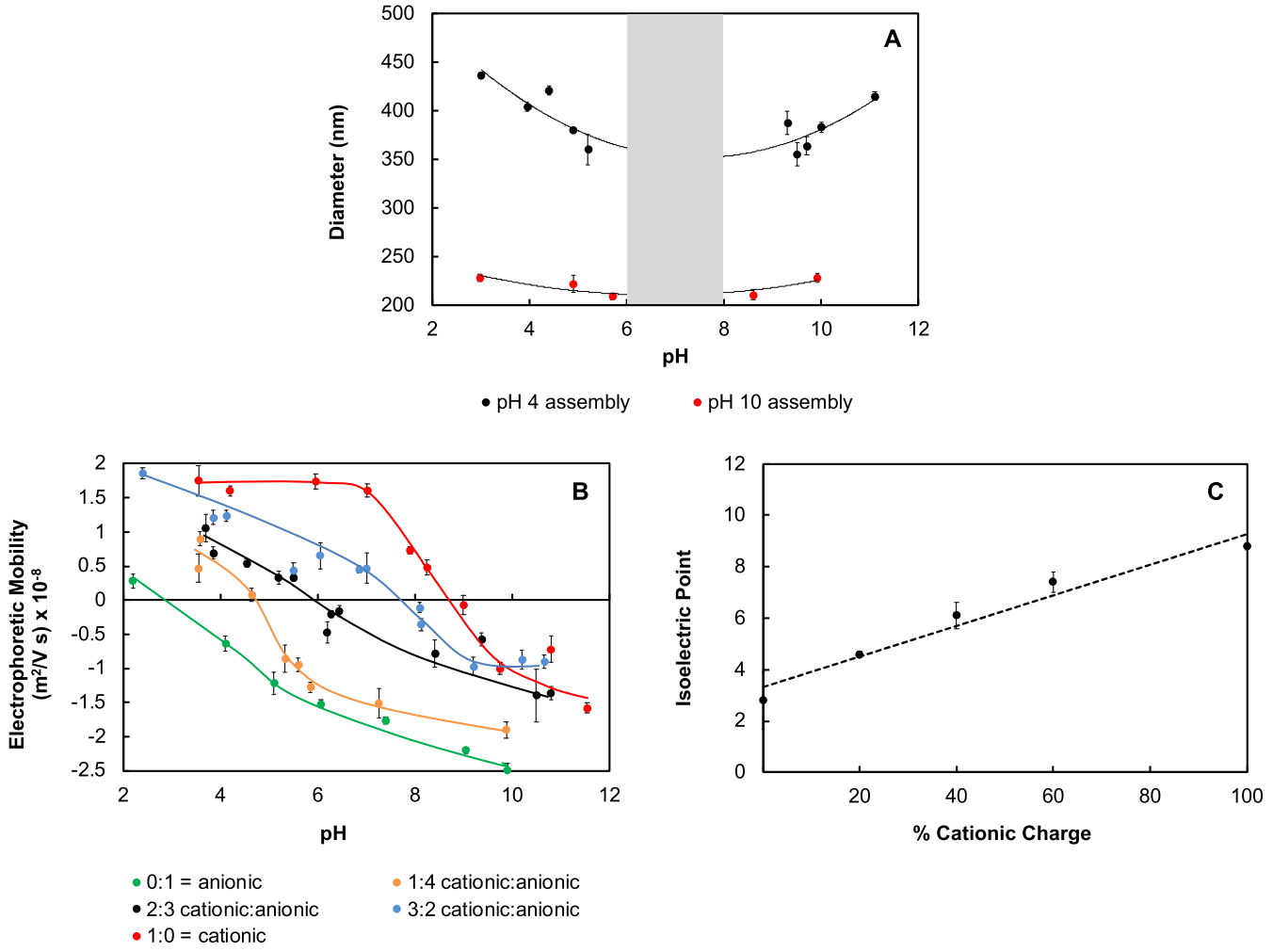

Figure 4. (A) Diameter versus pH measurements for amphoteric (+)/(−)-PNIPAM-Hzd (1:1 ratio)/(0)-PNIPAM-Ald self-assembled PNIPAM microgels prepared in 5 mM NaCl at self-assembly pH values of 4 or 10; (B) electrophoretic mobility versus pH measurements for amphoteric self-assembled PNIPAM microgels prepared in 5 mM NaCl using different mass ratios of (+)-PNIPAM-Hzd to (−)-PNIPAM-Hzd as the seed polymer (lines are guides to the eye); (C) isoelectric point of amphoteric self-assembled PNIPAM microgels as a function of percentage of (+)-PNIPAM-Hzd precursor polymer used to fabricate the microgel (the remainder of the polymer being (−)-PNIPAM-Hzd).

observed for the double cationic cross-linking system, with assemblies performed at pH 10 (both polymers uncharged) resulting in larger particle sizes, while assemblies performed at pH 7 (both polymers partially charged) resulting in smaller particles (~200 nm). Using cationic polymer only as the cross-linking polymer ((0)-PNIPAM-Hzd/(+)-PNIPAM-Ald) results in the production of microgels with lower electrophoretic mobilities and lower pH-induced deswelling responses as the pH is increased, consistent with the lower total charge content of these microgels given the 1:5 mass ratio between the cross-linker:seed polymer masses during self-assembly; however, similarly higher sizes (300−450 nm) and polydispersities (0.25−0.35) to the double cationic polymer system were observed. Overall, the data suggest that using the neutral aldehyde polymer cross-linker (whose cloud point is substantially lower than that of the cationic aldehyde polymer across any partially ionized pH value; Table 2) results in more pH-responsive and much more monodisperse microgel populations. We hypothesize that the neutral aldehyde polymer is a better steric stabilizer and thus can better prevent interparticle aggregation during the cross-linking process.

Anionic PNIPAM Microgels. Analogous to the cationic self-assembled PNIPAM microgels, anionic self-assembled PNIPAM microgels were fabricated using the self-assembly method at a temperature of 5 °C + cloud point of the hydrazide (seed) polymer, with the resulting microgel properties shown in Figure 3. In this case, consistent with conventional anionic microgels, the hydrodynamic diameter increases as a function of pH (consistent with the pK_a ~ 4.25 of the anionic acrylic acid comonomer[34]); correspondingly, the electrophoretic mobility of the microgels was neutral at acidic pH values and increasingly anionic as the pH was increased. Consistent with results shown for the self-assembled cationic microgels (Figure 2), the (−)-PNIPAM-Hzd/(0)-PNIPAM-Ald microgels (ionic seed polymer, neutral cross-linking polymer) self-assembled at a pH at which the acrylic acid residues were ionized (pH 7 or pH 10) exhibited substantially lower polydispersity and higher reproducibility than if an ionic polymer cross-linker is used, regardless of whether the seed polymer is charged. Indeed, the relatively low polydispersities (0.07−0.14) achieved under this self-assembly condition suggest the potential of the self-assembly method to create well-defined microgel populations even when functionalization

https://dx.doi.org/10.1021/acs.macromol.0c02304
Macromolecules 2021, 54, 351−363

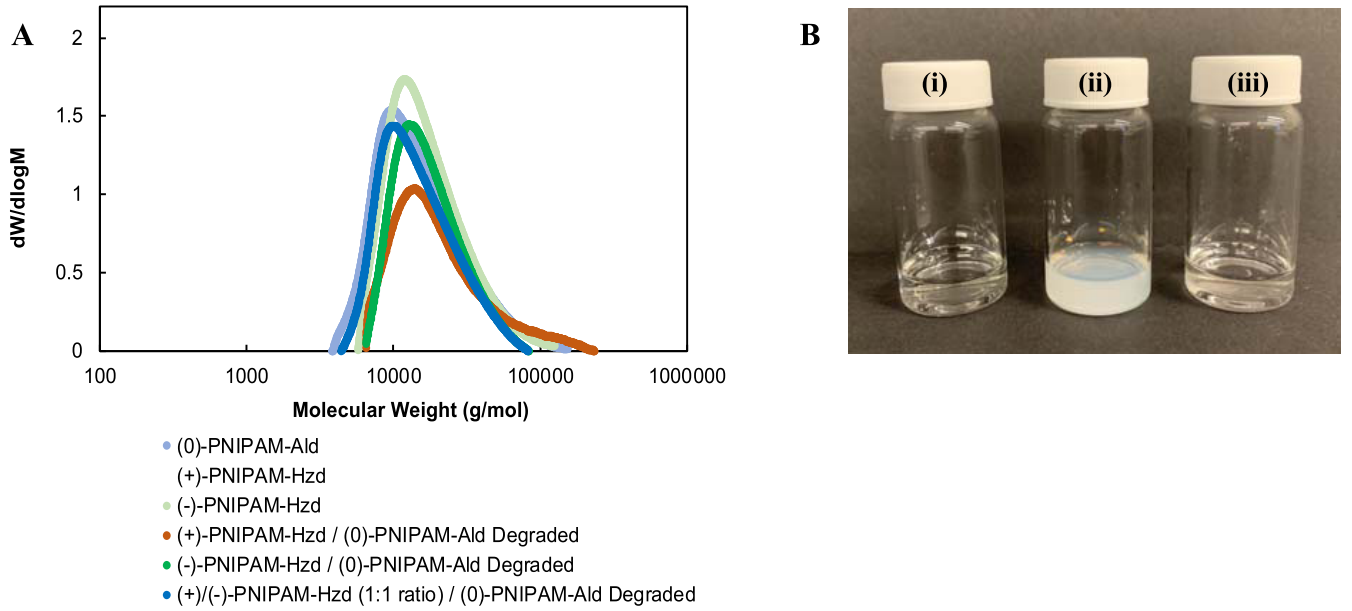

Figure 5. (A) Molecular weight distributions (relative to PEG calibration standards) of the precursor polymers and the degradation products from microgel hydrolysis after 24 h of exposure time to 1 M HCl for charged self-assembled PNIPAM microgels, and (B) representative images of the precursor (+)-Hzd polymer (i), self-assembled (+)-PNIPAM-Hzd/(0)-PNIPAM-Ald microgels (ii), and the degraded (+)-PNIPAM-Hzd/(0)-PNIPAM-Ald microgels after 24 h of exposure to 1 M HCl (iii).

is introduced. The absolute sizes achieved with anionic self-assembly are also much lower than those achieved using cationic self-assembly, a result we attribute to the improved electrostatic stabilization provided by anionic functional groups in the presence of the background salt.[51]

Amphoteric Microgels. The "mix-and-match" nature of hydrazone cross-linking allows for the fabrication of amphoteric microgels by simply mixing cationic and anionic hydrazide-functionalized precursor polymers. This seed polymer blending approach is advantageous relative to chemically synthesizing a hydrazide precursor polymer containing both cationic and anionic charges in that the same polymers used for single-charge microgel fabrication can be used to fabricate amphoteric microgels with any desired charge ratio by simple mixing. Given the polyelectrolyte interactions between cationic and anionic precursor polymers that can lead to coacervate formation in water, a 5 mM NaCl background salt solution was used for all assemblies to partially screen such coacervation and promote the formation of more stable microgel particles. Figure 4A shows the resulting diameter versus pH profiles of amphoteric (+)/(−)-PNIPAM-Hzd (1:1 ratio)/(0)-PNIPAM-Ald microgels self-assembled at pH 4 or pH 10. In both cases, the diameter followed a U-shaped profile as a function of pH, analogous to conventional precipitation PNIPAM microgels,[52] with aggregation due to charge coacervation (indicated by the gray box) observed ± 1 pH unit from neutral pH (expected to be the isoelectric point of the equal charge amphoteric microgel). Assemblies at pH 4 (cationic polymer charged, anionic polymer neutral) result in microgels with sizes and polydispersities similar to those achieved when only cationic seed polymers are used at the same pH (Figure 2); similarly, assemblies at pH 10 (anionic polymer charged, cationic polymer neutral) yield microgels with sizes similar to those produced with only anionic precursor polymers at the same pH (Figure 3). Thus, the polymer that introduces charge into the nanoaggregate appears to govern the properties of the resulting microgels produced.

Figure 4B shows the corresponding electrophoretic mobility as a function of pH for cationic, anionic, and amphoteric self-assembled microgels using (0)-PNIPAM-Ald as the cross-linker (the condition consistently leading to the lowest polydispersity microgels in Figures 2 and 3) and a 0.20 Ald:Hzd ratio in 5 mM NaCl at 70 °C without any pH adjustment during assembly.

Cationic microgels were fully charged at low pH, while anionic microgels were fully charged at high pH, consistent with the different pK_a values of the comonomers. The self-assembled amphoteric PNIPAM microgel prepared at a 1:1 cationic:anionic charge ratio had intermediate electrophoretic mobility values with an isoelectric point of ∼7, consistent with the aggregation results observed in the particle size curve (Figure 4A). Electrophoretic mobility measurements as a function of pH demonstrate that changing the ratio of (+)-PNIPAM-Hzd and (−)-PNIPAM-Hzd used as the seed polymer can lead to microgels with different cationic:anionic charge ratios and thus isoelectric points (Figure 4B). Isoelectric points of 4.6, 6.3, and 8.1 were observed for (+):(−) charge ratios 1:4, 2:3, and 3:2, respectively, yielding a nearly linear correlation between the cation/anion ratio and the isoelectric point (Figure 4C). Consequently, instead of synthesizing a conventional microgel with defined amounts of anionic and cationic charges for each desired charge ratio, the self-assembly of varying ratios of cationic and anionic seed polymer can achieve well-controlled amphoteric microgels of any charge density/ratio based on mixing a defined number of functionalized precursor polymers using a fast (∼10 min) assembly process.

Degradation. To assess the ability of these charged self-assembled PNIPAM microgels to degrade back into the precursor polymer (as observed with the uncharged self-assembled microgels[34]), the single-charge (+)-PNIPAM-Hzd/(0)-PNIPAM-Ald and (−)-PNIPAM-Hzd/(0)-PNIPAM-Ald as well as amphoteric (+)/(−)-PNIPAM-Hzd (1:1 ratio)/(0)-PNIPAM-Ald microgels were exposed to 1 M HCl to perform

https://dx.doi.org/10.1021/acs.macromol.0c02304
Macromolecules 2021, 54, 351−363

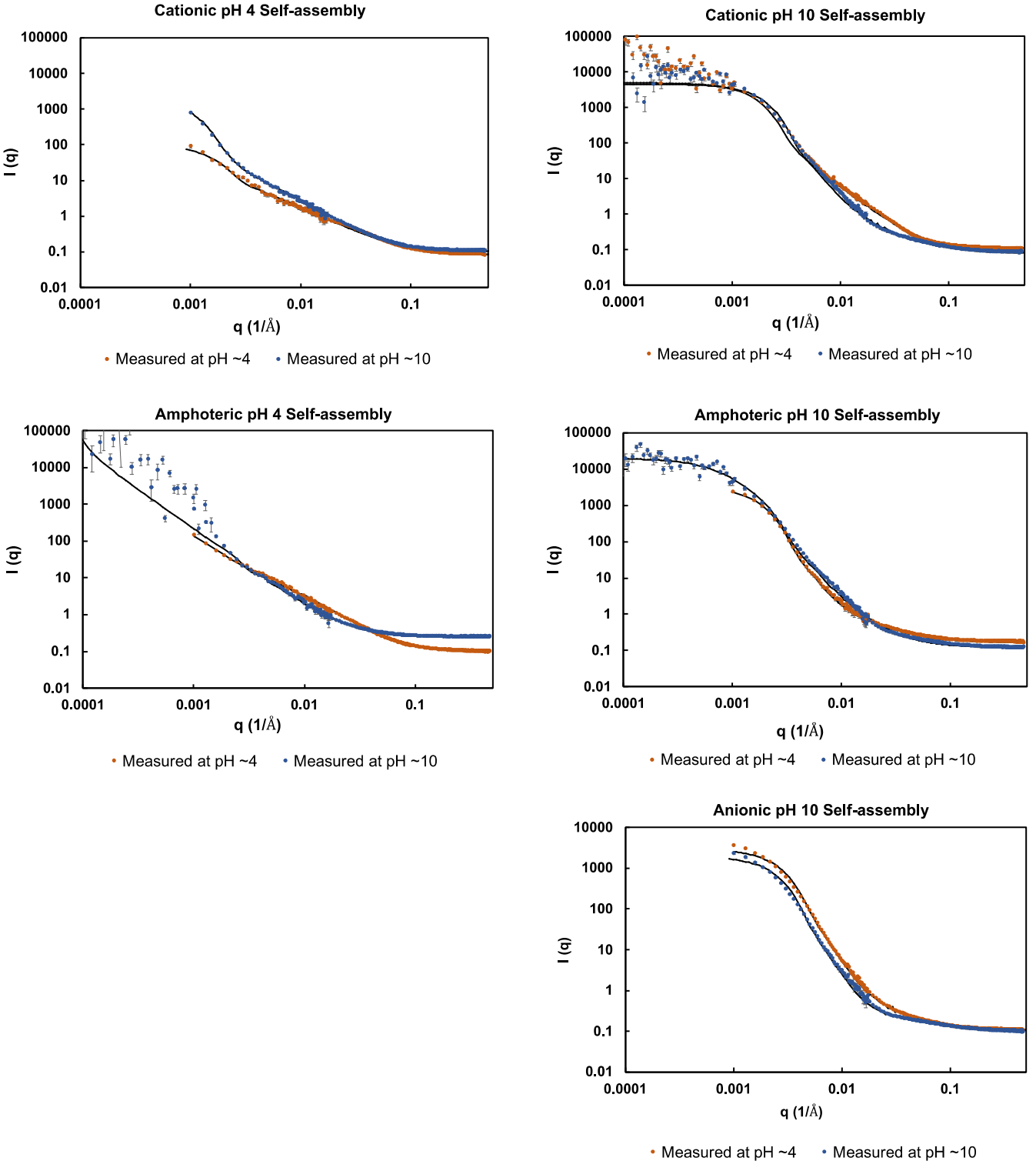

Figure 6. SANS and USANS scattering profiles for charged self-assembled PNIPAM microgels cross-linked using a neutral PNIPAM-Ald precursor polymer assembled at pH 4 or pH 10 and subsequently measured at pH 4 or pH 10.

an accelerated degradation. Figure 5A shows the molecular weight distributions (measured against PEG standards) of both the original precursor polymers and the degradation products from the microgel hydrolysis after 24 h of exposure time. While a small tail at higher molecular weights was observed for the degraded cationic microgel (consistent with the potential charge repulsion between the polymer and the H+ degradation catalyst), the results show successful cleavage of the microgels back into the starting PNIPAM-Ald and (+,−) PNIPAM-Hzd precursor polymers; each of the precursor polymers and degradation products has a mode between ∼19 and 20 kDa. This molecular weight trend is consistent with the visual appearance of the microgels, with the fully soluble precursors creating translucent microgel suspensions upon self-assembly that return to transparent solutions following degradation (Figure 5B); see the Supporting Information Figure S7 for

https://dx.doi.org/10.1021/acs.macromol.0c02304
Macromolecules 2021, 54, 351−363

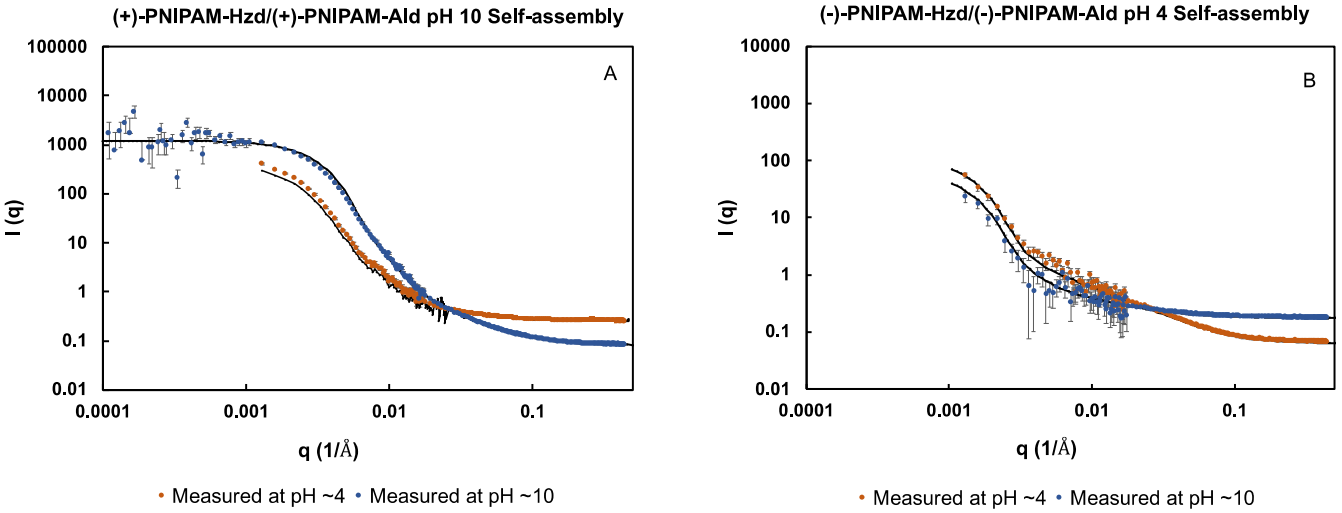

Figure 7. SANS and USANS scattering profiles for charged self-assembled PNIPAM microgels cross-linked using the same charged PNIPAM-Ald precursor polymer assembled at a pH value at which both precursor polymers are nonionized.

corresponding pictures of other microgels and their degradation products. As such, the charged microgels can degrade back into clearable lower-molecular-weight products over time.

Internal Morphology. To assess the internal morphology of the self-assembled microgels, assemblies were repeated in D_2O (with pH adjusted to 4 or 10 using 0.1 M NaOH or HCl as previously described) to enable neutron scattering contrast; anionic microgels self-assembled at pH 4 were omitted due to the previously described aggregation observed in those samples. The resulting microgels were subsequently characterized at low and high pH (corresponding to their fully charged or fully neutral states) using small-angle neutron scattering (SANS) and, in some cases in which curve fitting was challenging with the q range of SANS, ultrasmall-angle neutron scattering (USANS). The neutron scattering curves of microgels cross-linked with neutral PNIPAM-Ald (i.e., formulations that consistently yielded the smallest and most monodisperse microgels, as per Figures 2, 3, and 4—4) are shown in Figure 6 (see the Supporting Information Table S2 for best-fit parameters).

Unlike the uncharged self-assembled PNIPAM microgels,[35] the charged self-assembled PNIPAM microgels required two different models to fit the scattering profiles depending on the charges present, demonstrating that the internal morphology of these microgels differs depending on the charge interactions. Anionic and cationic self-assembled PNIPAM microgels were successfully fit according to a homogeneously cross-linked internal structure, as per the neutral microgels; however, amphoteric self-assembled PNIPAM microgels required an additional weak interaction modeled as a square well potential to enable proper fits. This interaction factor, previously used to model electrostatic interactions in hard-sphere systems,[45] is required to accurately model the additional electrostatic interactions (and thus the presence of local charge domains within the otherwise radially homogeneous structure) between the oppositely charged seed precursor polymers that are only present in the amphoteric PNIPAM microgels.

Microgels fabricated with a charged cross-linker yielded less regular scattering curves, consistent with the significantly higher polydispersities observed for most of these microgels. For the double charge microgels, only the (+)-PNIPAM-Hzd/(+)-PNIPAM-Ald microgel assembled at pH 10 and the (−)-PNIPAM-Hzd/(−)-PNIPAM-Ald microgel assembled at pH 4 produced reproducible (nonaggregating) scattering curves, as shown in Figure 7 (see the Supporting Information Figure S8 for scattering curves from other assembly pH values for the double charge microgel system). Both these conditions are those in which the charged precursor polymer has no net charge (and thus a lower temperature and much more discontinuous phase transition) under the assembly conditions (Supporting Figure S6). This result is also consistent with the lower polydispersities observed in the dynamic light scattering (DLS) data for these microgels (Figures 2 and 3).

Considered together, low polydispersity and homogeneous network single-charge self-assembled microgels are best prepared from systems in which (1) the seed polymer undergoes a clear phase transition prior to cross-linker addition and (2) a cross-linking polymer is used that is uncharged at the assembly conditions. Note that the microgels produced using any assembly condition that produced well-defined microgels based on the above criteria could be successfully fit using a homogeneous sphere model without requiring the consideration of a "fuzzy" outer layer (albeit also requiring the incorporation of a square well potential for the amphoteric microgels to capture the charge interaction effects on the initial nanoaggregate structure). As such, the tendency of self-assembled microgels to form homogeneous microgels can be maintained even in the presence of charged precursor polymers. In contrast, using a cross-linking polymer (particularly the one with the opposite charge of the seed polymer) typically results in highly aggregative structures that are difficult to fit with any model (see the Supporting Information Figure S9 and Table S3). While charge interactions to form the initial nanoaggregate can be successfully managed under the right assembly conditions (i.e., using charge to effectively internally cross-link the nanoaggregate without inducing a loss of colloidal stability), charge interactions between the cross-linking and seed polymers under the assembly conditions must be avoided to maintain sufficient stability between the nanoaggregates and produce reproducible monodisperse microgels.

Cell Cytotoxicity. To confirm the potential use of these degradable self-assembled microgels in biomedical applications, the cytotoxicity of anionic, cationic, and amphoteric

https://dx.doi.org/10.1021/acs.macromol.0c02304
Macromolecules 2021, 54, 351−363

microgels fabricated under the optimal fabrication conditions (i.e., neutral (0)-PNIPAM-Ald cross-linker, pH 7) was assessed via the MTS assay using C2C12 mouse myoblast cells. Figure 8

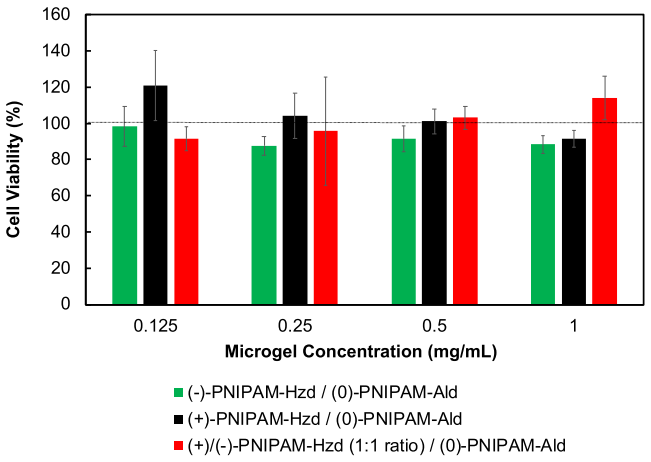

Figure 8. C2C12 cell viability (relative to a cell-only control) of charged self-assembled PNIPAM microgels cross-linked with neutral PNIPAM-Ald precursor polymer assembled and tested at pH 7.

shows that all of the self-assembled microgels tested (regardless of charge) maintained high cytocompatibility, with cell viabilities of >80% observed at all microgel concentrations tested. In particular, despite the reported cytotoxicity of some cationic microgels,[53−55] no significant decrease in cell viability was observed for the cationic self-assembled PNIPAM microgels, suggesting their potentially safer use in biomedical applications. Coupling this result with the dual microenvironment-responsive nature of the charged microgels (Figures 2 and 3) and the demonstrated degradability of these self-assembled microgels (Figure 5), we anticipate future utility for such microgels for drug delivery applications.

CONCLUSIONS

Charged self-assembled PNIPAM microgels can be fabricated by functionalizing the precursor hydrazide and aldehyde PNIPAM polymers with DMAEMA and AA to introduce cationic and anionic charges, respectively. Cationic single-charged PNIPAM microgels deswell as a function of pH, while the anionic single-charged PNIPAM microgels swell as a function of pH, consistent with the pK_a values of the respective functional monomers and analogous to observations with conventional precipitation-based PNIPAM microgels. Amphoteric self-assembled PNIPAM microgels can similarly be fabricated by using a mixture of cationic and anionic PNIPAM-Hzd as the seed polymer in the self-assembly, resulting in microgels with U-shaped diameter versus pH curves and an isoelectric point of pH ∼ 7; different cationic:anionic charge density microgels can similarly be produced to result in any desired isoelectric point or swelling profile by simply mixing different ratios of the cationic and anionic PNIPAM-Hzd precursor polymers, offering a high level of control over microgel deswelling and/or aggregation at any specific pH/temperature combination without requiring the "from-scratch" synthesis of distinct microgels as required with the conventional precipitation polymerization synthetic route. The microgel properties achieved are directly analogous to those achievable with conventional precipitation-based microgels while also offering the potential for degradation back into low-molecular-weight precursor polymers via hydrazone cross-link hydrolysis over time. This combination of desirable pH swelling responses and degradability suggests the potential use of these charged self-assembled PNIPAM microgels in applications including ion exchange, drug delivery (particularly in terms of targeting infection sites or rapidly metabolizing tumor sites that are characterized by higher local temperature and lower local pH), and environmental sorption.

ASSOCIATED CONTENT

Supporting Information

The Supporting Information is available free of charge at https://pubs.acs.org/doi/10.1021/acs.macromol.0c02304.

^{1}H NMR spectra of the acrylate hydrazide monomer and the four charged hydrazide or aldehyde-functionalized precursor polymers, cloud point curves over the full scanned temperature range using UV−vis spectrophotometry, and SANS/USANS data for same charge cross-linker/seed polymer and opposite charge cross-linker/seed polymer microgel assemblies are provided (PDF)

AUTHOR INFORMATION

Corresponding Author

Todd Hoare − *Department of Chemical Engineering, McMaster University, Hamilton, Ontario, Canada L8S 4L7;* orcid.org/0000-0002-5698-8463; Email: hoaretr@mcmaster.ca

Authors

Eva Mueller − *Department of Chemical Engineering, McMaster University, Hamilton, Ontario, Canada L8S 4L7*

Sebastian Himbert − *Department of Physics and Astronomy, McMaster University, Hamilton, Ontario, Canada L8S 4M1*

Madeline J. Simpson − *Department of Chemical Engineering, McMaster University, Hamilton, Ontario, Canada L8S 4L7*

Markus Bleuel − *NIST Center for Neutron Research, National Institute of Standards and Technology, Gaithersburg, Maryland 20899-3460, United States; Department of Materials Science and Engineering, University of Maryland, College Park, Maryland 20742-2115, United States*

Maikel C. Rheinstadter − *Department of Physics and Astronomy, McMaster University, Hamilton, Ontario, Canada L8S 4M1;* orcid.org/0000-0002-0558-7475

Complete contact information is available at: https://pubs.acs.org/10.1021/acs.macromol.0c02304

Notes

Specific commercial equipment, instruments, or materials are identified in this paper to foster understanding. Such identification does not imply recommendation or endorsement by the National Institute of Standards and Technology nor does it imply that the materials or equipment identified are necessarily the best available for the purpose.

The authors declare no competing financial interest.

ACKNOWLEDGMENTS

The Natural Sciences and Engineering Research Council of Canada (NSERC, RGPIN-06455-2017) is gratefully acknowledged for funding. Access to the SANS NGB30 and BT5 USANS instruments was provided by the Center for High Resolution Neutron Scattering, a partnership between the

National Institute of Standards and Technology and the National Science Foundation under Agreement No. DMR-1508249. We acknowledge the support of the National Institute of Standards and Technology, U.S. Department of Commerce, in providing the neutron research facilities used in this work and the support and help from Cedric Gagnon at the SANS NGB30 and BT5 USANS instruments. Ridhdhi Dave, Gero Padberg, Terrel Marshall, Albert Sadowski, Lukas Sadowski, and Zhicheng Pan are gratefully acknowledged for their collaboration on this project.

REFERENCES

(1) Roth, P. J.; Lowe, A. B. Stimulus-responsive polymers. *Polym. Chem.* **2017**, *8*, 10−11.
(2) Galaev, I. Y.; Mattiasson, B. 'Smart'polymers and what they could do in biotechnology and medicine. *Trends Biotechnol.* **1999**, *17*, 335−340.
(3) Aguilar, M. R.; Elvira, C.; Gallardo, A.; Vázquez, B.; Román, J., Smart polymers and their applications as biomaterials. *Top. Tissue Eng.* **2007**, *3* ().
(4) Soppimath, K. S.; Aminabhavi, T. M.; Dave, A. M.; Kumbar, S. G.; Rudzinski, W. Stimulus-responsive "smart" hydrogels as novel drug delivery systems. *Drug Dev. Ind. Pharm.* **2002**, *28*, 957−974.
(5) Qiu, Y.; Park, K. Environment-sensitive hydrogels for drug delivery. *Adv. Drug Delivery Rev.* **2001**, *53*, 321−339.
(6) Hoare, T. R.; Kohane, D. S. Hydrogels in drug delivery: Progress and challenges. *Polymer* **2008**, *49*, 1993−2007.
(7) Hajebi, S.; Rabiee, N.; Bagherzadeh, M.; Ahmadi, S.; Rabiee, M.; Roghani-Mamaqani, H.; Tahriri, M.; Tayebi, L.; Hamblin, M. R. Stimulus-responsive polymeric nanogels as smart drug delivery systems. *Acta Biomater.* **2019**, *92*, 1−18.
(8) Karimi, M.; Ghasemi, A.; Zangabad, P. S.; Rahighi, R.; Basri, S. M. M.; Mirshekari, H.; Amiri, M.; Pishabad, Z. S.; Aslani, A.; Bozorgomid, M.; et al. Smart micro/nanoparticles in stimulus-responsive drug/gene delivery systems. *Chem. Soc. Rev.* **2016**, *45*, 1457−1501.
(9) Agrawal, G.; Agrawal, R. Stimuli-responsive microgels and microgel-based systems: Advances in the exploitation of microgel colloidal properties and their interfacial activity. *Polymers* **2018**, *10*, 418.
(10) Guan, Y.; Zhang, Y. PNIPAM microgels for biomedical applications: from dispersed particles to 3D assemblies. *Soft Matter* **2011**, *7*, 6375−6384.
(11) Plamper, F. A.; Richtering, W. Functional microgels and microgel systems. *Acc. Chem. Res.* **2017**, *50*, 131−140.
(12) Pelton, R.; Chibante, P. Preparation of aqueous latices with N-isopropylacrylamide. *Colloids Surf.* **1986**, *20*, 247−256.
(13) McMasters, J.; Poh, S.; Lin, J. B.; Panitch, A. Delivery of anti-inflammatory peptides from hollow PEGylated poly (NIPAM) nanoparticles reduces inflammation in an ex vivo osteoarthritis model. *J. Controlled Release* **2017**, *258*, 161−170.
(14) Xu, W.; Zhang, Y.; Gao, Y.; Serpe, M. J. Electrically triggered small molecule release from poly (n-isopropylacrylamide-co-acrylic acid) microgel-modified electrodes. *ACS Appl. Mater. Interfaces* **2018**, *10*, 13124−13129.
(15) Kim, Y. K.; Kim, E.-J.; Lim, J. H.; Cho, H. K.; Hong, W. J.; Jeon, H. H.; Chung, B. G. Dual stimuli-triggered nanogels in response to temperature and pH changes for controlled drug release. *Nanoscale Res. Lett.* **2019**, *14*, No. 77.
(16) Kratz, K.; Hellweg, T.; Eimer, W. Influence of charge density on the swelling of colloidal poly (N-isopropylacrylamide-co-acrylic acid) microgels. *Colloids Surf., A* **2000**, *170*, 137−149.
(17) Kokufuta, E.; Wang, B.; Yoshida, R.; Khokhlov, A. R.; Hirata, M. Volume phase transition of polyelectrolyte gels with different charge distributions. *Macromolecules* **1998**, *31*, 6878−6884.
(18) Morris, G. E.; Vincent, B.; Snowden, M. J. Adsorption of lead ions ontoN-Isopropylacrylamide and acrylic acid copolymer microgels. *J. Colloid Interface Sci.* **1997**, *190*, 198−205.
(19) Brändel, T.; Wiehemeier, L.; Kottke, T.; Hellweg, T. Microphase separation of smart double-responsive copolymer microgels studied by local fluorescence probes. *Polymer* **2017**, *125*, 110−116.
(20) Zhou, S.; Chu, B. Synthesis and volume phase transition of poly (methacrylic acid-co-N-isopropylacrylamide) microgel particles in water. *J. Phys. Chem. B* **1998**, *102*, 1364−1371.
(21) Dowding, P. J.; Vincent, B.; Williams, E. Preparation and swelling properties of poly (NIPAM)"minigel" particles prepared by inverse suspension polymerization. *J. Colloid Interface Sci.* **2000**, *221*, 268−272.
(22) Marcelo, G.; Areias, L. R.; Viciosa, M. T.; Martinho, J.; Farinha, J. P. S. PNIPAm-based microgels with a UCST response. *Polymer* **2017**, *116*, 261−267.
(23) Dhanya, S.; Bahadur, D.; Kundu, G.; Srivastava, R. Maleic acid incorporated poly-(N-isopropylacrylamide) polymer nanogels for dual-responsive delivery of doxorubicin hydrochloride. *Eur. Polym. J.* **2013**, *49*, 22−32.
(24) Hoare, T.; Pelton, R. Highly pH and temperature responsive microgels functionalized with vinylacetic acid. *Macromolecules* **2004**, *37*, 2544−2550.
(25) Karg, M.; Pastoriza-Santos, I.; Rodriguez-Gonzalez, B.; von Klitzing, R.; Wellert, S.; Hellweg, T. Temperature, pH, and ionic strength induced changes of the swelling behavior of PNIPAM− poly (allylacetic acid) copolymer microgels. *Langmuir* **2008**, *24*, 6300−6306.
(26) Echeverría, C.; Aragón-Gutiérrez, A.; Fernández-García, M.; Muñoz-Bonilla, A.; López, D. Thermoresponsive poly (N-isopropylacrylamide-co-dimethylaminoethyl methacrylate) microgel aqueous dispersions with potential antimicrobial properties. *Polymers* **2019**, *11*, 606.
(27) Ahiabu, A.; Serpe, M. J. Rapidly responding pH-and temperature-responsive poly (N-Isopropylacrylamide)-based microgels and assemblies. *ACS Omega* **2017**, *2*, 1769−1777.
(28) Karg, M.; Hellweg, T. New "smart" poly (NIPAM) microgels and nanoparticle microgel hybrids: Properties and advances in characterisation. *Curr. Opin. Colloid Interface Sci.* **2009**, *14*, 438−450.
(29) Debord, J. D.; Lyon, L. A. Synthesis and characterization of pH-responsive copolymer microgels with tunable volume phase transition temperatures. *Langmuir* **2003**, *19*, 7662−7664.
(30) Das, M.; Mardyani, S.; Chan, W. C.; Kumacheva, E. Biofunctionalized pH-responsive microgels for cancer cell targeting: rational design. *Adv. Mater.* **2006**, *18*, 80−83.
(31) Smeets, N. M.; Hoare, T. Designing responsive microgels for drug delivery applications. *J. Polym. Sci., Part A: Polym. Chem.* **2013**, *51*, 3027−3043.
(32) Gao, J.; Frisken, B. J. Cross-linker-free N-isopropylacrylamide gel nanospheres. *Langmuir* **2003**, *19*, 5212−5216.
(33) Bachman, H.; Brown, A. C.; Clarke, K. C.; Dhada, K. S.; Douglas, A.; Hansen, C. E.; Herman, E.; Hyatt, J. S.; Kodlekere, P.; Meng, Z.; et al. Ultrasoft, highly deformable microgels. *Soft Matter* **2015**, *11*, 2018−2028.
(34) Sivakumaran, D.; Mueller, E.; Hoare, T. Temperature-induced assembly of monodisperse, covalently cross-linked, and degradable poly (N-isopropylacrylamide) microgels based on oligomeric precursors. *Langmuir* **2015**, *31*, 5767−5778.
(35) Mueller, E.; Alsop, R. J.; Scotti, A.; Bleuel, M.; Rheinstädter, M. C.; Richtering, W.; Hoare, T. Dynamically cross-linked self-assembled thermoresponsive microgels with homogeneous internal structures. *Langmuir* **2018**, *34*, 1601−1612.
(36) Schachschal, S.; Balaceanu, A.; Melian, C.; Demco, D. E.; Eckert, T.; Richtering, W.; Pich, A. Polyampholyte microgels with anionic core and cationic shell. *Macromolecules* **2010**, *43*, 4331−4339.
(37) Pich, A.; Richtering, W. Microgels by precipitation polymerization: synthesis, characterization, and functionalization. In *Chemical Design of Responsive Microgels*; Springer, 2010; pp 1−37.
(38) Ogawa, K.; Nakayama, A.; Kokufuta, E. Preparation and characterization of thermosensitive polyampholyte nanogels. *Langmuir* **2003**, *19*, 3178−3184.

https://dx.doi.org/10.1021/acs.macromol.0c02304
Macromolecules 2021, 54, 351−363

(39) Taira, S.; Du, Y. Z.; Kodaka, M. Trap and release of oligonucleotide using pH-responsive amphoteric particle prepared by interfacial polymerization in W/O miniemulsion system. *Biotechnol. Bioeng.* **2006**, *93*, 396−400.
(40) Das, M.; Mordoukhovski, L.; Kumacheva, E. Sequestering gold nanorods by polymer microgels. *Adv. Mater.* **2008**, *20*, 2371−2375.
(41) Glinka, C.; Barker, J.; Hammouda, B.; Krueger, S.; Moyer, J.; Orts, W. The 30 m small-angle neutron scattering instruments at the National Institute of Standards and Technology. *J. Appl. Crystallogr.* **1998**, *31*, 430−445.
(42) Kline, S. R. Reduction and analysis of SANS and USANS data using IGOR Pro. *J. Appl. Crystallogr.* **2006**, *39*, 895−900.
(43) Azuah, R. T.; Kneller, L. R.; Qiu, Y.; Tregenna-Piggott, P. L.; Brown, C. M.; Copley, J. R.; Dimeo, R. M. DAVE: a comprehensive software suite for the reduction, visualization, and analysis of low energy neutron spectroscopic data. *J. Res. Natl. Inst. Stand. Technol.* **2009**, *114*, 341.
(44) Barker, J.; Glinka, C.; Moyer, J.; Kim, M.; Drews, A.; Agamalian, M. Design and performance of a thermal-neutron double-crystal diffractometer for USANS at NIST. *J. Appl. Crystallogr.* **2005**, *38*, 1004−1011.
(45) Sharma, R.; Sharma, K. The structure factor and the transport properties of dense fluids having molecules with square well potential, a possible generalization. *Phys. A* **1977**, *89*, 213−218.
(46) Wu, X.; Pelton, R.; Hamielec, A.; Woods, D.; McPhee, W. The kinetics of poly (N-isopropylacrylamide) microgel latex formation. *Colloid Polym. Sci.* **1994**, *272*, 467−477.
(47) Lin, W.; Ma, X.; Qian, J.; Abdelrahman, A. I.; Halupa, A.; Baranov, V.; Pich, A.; Winnik, M. A. Synthesis and mass cytometric analysis of lanthanide-encoded polyelectrolyte microgels. *Langmuir* **2011**, *27*, 7265−7275.
(48) Simpson, M. J.; Corbett, B.; Arezina, A.; Hoare, T. Narrowly dispersed, degradable, and scalable poly (oligoethylene glycol methacrylate)-based nanogels via thermal self-assembly. *Ind. Eng. Chem. Res.* **2018**, *57*, 7495−7506.
(49) Kolev, S. K.; Petkov, P. S.; Rangelov, M. A.; Vayssilov, G. N. Density functional study of hydrogen bond formation between methanol and organic molecules containing Cl, F, NH2, OH, and COOH functional groups. *J. Phys. Chem. A* **2011**, *115*, 14054−14068.
(50) Bernal, J. D.; Fowler, R. H. A theory of water and ionic solution, with particular reference to hydrogen and hydroxyl ions. *J. Chem. Phys.* **1933**, *1*, 515−548.
(51) Perez-Jimenez, R.; Godoy-Ruiz, R.; Ibarra-Molero, B.; Sanchez-Ruiz, J. M. The efficiency of different salts to screen charge interactions in proteins: a Hofmeister effect? *Biophys. J.* **2004**, *86*, 2414−2429.
(52) Ni, H.; Kawaguchi, H.; Endo, T. Preparation of Amphoteric Microgels of Poly (acrylamide/methacrylic acid/dimethylamino ethylene methacrylate) with a Novel pH− Volume Transition. *Macromolecules* **2007**, *40*, 6370−6376.
(53) Fröhlich, E. The role of surface charge in cellular uptake and cytotoxicity of medical nanoparticles. *Int. J. Nanomed.* **2012**, *7*, 5577.
(54) Chen, L.; Simpson, J. D.; Fuchs, A. V.; Rolfe, B. E.; Thurecht, K. J. Effects of surface charge of hyperbranched polymers on cytotoxicity, dynamic cellular uptake and localization, hemotoxicity, and pharmacokinetics in mice. *Mol. Pharmaceutics* **2017**, *14*, 4485−4497.
(55) Hörtz, C.; Birke, A.; Kaps, L.; Decker, S.; Wächtersbach, E.; Fischer, K.; Schuppan, D.; Barz, M.; Schmidt, M. Cylindrical brush polymers with polysarcosine side chains: a novel biocompatible carrier for biomedical applications. *Macromolecules* **2015**, *48*, 2074−2086.

https://dx.doi.org/10.1021/acs.macromol.0c02304
Macromolecules 2021, 54, 351−363